

Received September 10, 2019, accepted September 29, 2019, date of publication October 21, 2019, date of current version November 6, 2019.

Digital Object Identifier 10.1109/ACCESS.2019.2948785

Research on Vibration Control of Seating System Platform Based on the Cubic Stewart Parallel Mechanism

FENGRONG BI¹, TENG MA¹, XU WANG², XIAO YANG¹, AND ZHENPENG LV¹

¹State Key Laboratory of Engines, Tianjin University, Tianjin 300072, China

²School of Engineering, RMIT University, Melbourne, VIC 3001, Australia

Corresponding author: Teng Ma (mt258@tju.edu.cn)

This work was supported by International Cooperation Project for RMIT and Tianjin University Joint Research Center: Investigation of Low Frequency Idle Vibration and Lumpiness Control of Commercial Vehicle Driver's Seat through Passive and Semi-active Control Technologies.

ABSTRACT A multi-degree-of-freedom seating system platform based on the cubic Stewart parallel mechanism is designed for vibration control of an off-road vehicle driver's seat. A parameter sensitivity analysis is conducted to identify the most sensitive parameters for the transmissibility ratio of the seating system platform. Then, a vibration control method combining active and passive control for each branch of the seat platform leg is developed to reduce the driver's body vibration. The results indicate that the seating system platform designed in this article can reduce the vibration in the vertical direction, horizontal direction and roll direction simultaneously through passive vibration control. The vibration can be further reduced in these three directions by adding active vibration control.

INDEX TERMS Multi-degree-of-freedom vibration control, cubic Stewart parallel mechanism, sensitivity analysis, active vibration control.

I. INTRODUCTION

Off-road vehicles such as mining vehicles, tractors, and construction machinery are often used on non-paved roads. Due to the complex vibration displacement excitation from the uneven ground, the ride comfort of these vehicles is seriously affected. High-frequency vibration can be quickly attenuated by tire and vehicle suspension, while the low-frequency vibration (which has a greater impact on the human body) can be transmitted to the driver or passengers through the vehicle floor and seats. Long-term exposure to the low-frequency vibration environment causes driver's fatigue and a slow reaction time, which can lead to traffic accidents [1], [2]. Therefore, the research of seating system vibration reduction is very important for improving the driving comfort of off-road vehicles.

Conventional seating suspension design of road vehicles considers only the vertical vibration isolation. However, for off-road vehicles, the road conditions of these vehicles are very poor. The serious rolling vibration caused by the rough road surface greatly reduces the ride comfort of the vehicle.

The associate editor coordinating the review of this manuscript and approving it for publication was Ning Sun¹.

A half-car model with chassis suspension and seating suspension is shown in Fig. 1. In this figure, m_l , m_r , m_v and m_b are the mass of the left-hand side tire, the right-hand side tire, the vehicle body and driver body, respectively; k and c are the corresponding stiffness and damping coefficients. Vertical vibrations and rolling vibration around the x -axis of the vehicle chassis are transmitted through tires. Usually, the rolling vibration is too small to consider due to small road roughness. Reducing the vertical vibration of the seat greatly improves the ride comfort. In a poor road condition, as the road roughness increases, the rolling vibration magnitude also increases. In this situation, the driver body can be regarded as a mass at the top of an inverted pendulum system. Thus, high-magnitude lateral acceleration is caused by the rolling vibration [3].

In addition, the driving behavior (such as cornering, acceleration and obstacle avoidance) and other vibration excitation factors (including the engine, transmission system and wheels) also cause vibrations in multiple directions and degree of freedom. Therefore, the vehicle seating system should have a multi-degree-of-freedom (MDOF) vibration energy absorption function to improve the driver's comfort.

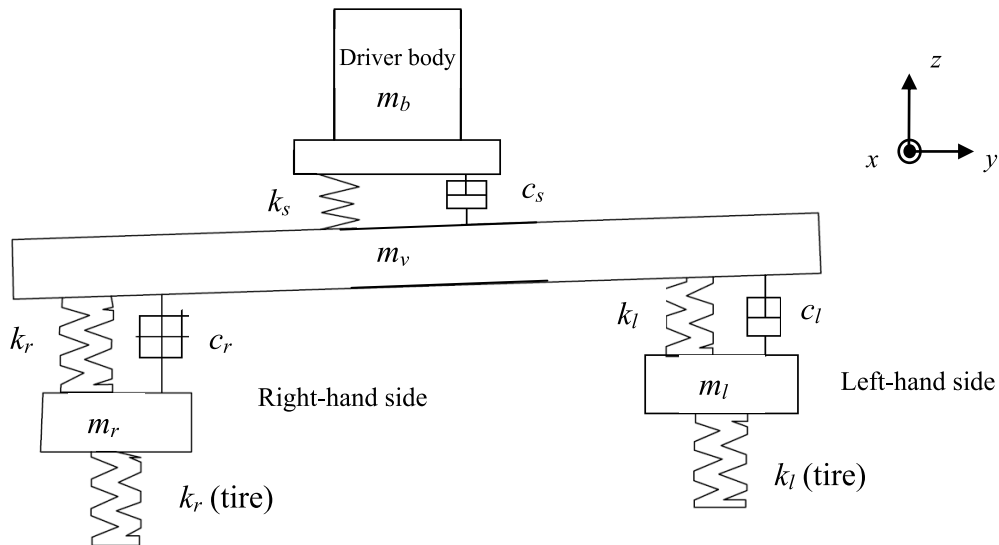


FIGURE 1. Half car model with chassis and seat suspension.

At present, commonly used multi-degree-of-freedom vibration absorption methods in engineering include the rubber shock absorber and mechanical vibration absorber. However, both the methods have disadvantages. Rubber products often suffer from poor performance under the harsh environments where off-road vehicles operate. For example, if the vibration amplitude is too large, the heat dissipation of rubber is aggravated, leading to damage to the rubber shock absorber. In addition, the rubber products have limited function because permanent deformation or even tearing can easily be produced by the large-amplitude vibration. When the mechanical vibration absorber is applied to multi-degree-of-freedom vibration absorption, the multilayer structure should be adapted accordingly. The structure of the vibration absorber is often very complex, and the moving parts can easily suffer from interference. The damping value is limited by the structure and dimension of the vibration absorber, so practical application is very inconvenient.

Parallel mechanisms have been applied in various fields because of a series of advantages. Parallel mechanisms can move in different directions at the same time, which can eliminate vibration in multiple degrees of freedom. Compared with conventional mechanical shock absorbers, parallel mechanisms do not need a multilayer structure and have higher reliability. As a classical parallel mechanism, the Stewart mechanism has the characteristics of large stiffness, strong load bearing capacity, small operating space and high control precision. In the past decades, many vibration absorption methods based on the Stewart mechanism have been proposed. Rahman proposed an orthogonal six-leg structure, which uses active control system to suppress the vibration of the space observation system. The experimental results showed that active vibration control can achieve additional vibration attenuation at 10 ~ 100 Hz compared

to the passive control [4]. Preumont *et al.* designed a six-axis vibration absorption system based on the Stewart mechanism and achieved good vibration reduction effect [5]. Cobb *et al.* invented a six-rod platform based on a hybrid vibration isolation mechanism to isolate and suppress vibration. This damping platform can effectively improve the performance of passive vibration isolation in the low-frequency range [6]. Behrouz Afzali-Far designed a Stewart parallel platform with symmetrical structure and studied the dynamic characteristics of the platform [7]. The Stewart platform also has been used in vehicle seat design [8].

Although Stewart platforms have unique advantages over traditional vibration control structures, the kinematic and dynamic analysis of the Stewart platform is complex. The primary problem with a general Stewart platform is that motions along different axes are strongly coupled, which means that motion in any Cartesian direction induces motion of all of the legs, resulting in mathematical complexity in control system design [9]. To solve this problem, a special-configuration Stewart platform, called the cubic Stewart platform, was first proposed as the architecture of a six-axis isolation system by Geng *et al.* [9].

The structure of this configuration is shown in Fig. 2. This picture shows the design principle of the cube configuration. On the basis of the cube, the two diagonals are removed by plane ABC and plane DEF. The two planes after removal are named as the load plane and foundation of the cube Stewart platform, while the six side lengths of the cube, AF, AE, BF, BD, CE and CD, become the six legs of the cubic Stewart platform [10].

The cube-configuration Stewart platform has many properties derived from cubes. In this Stewart platform type, the adjacent legs are orthogonal to each other, which can realize motion decoupling in three vertical axis directions.

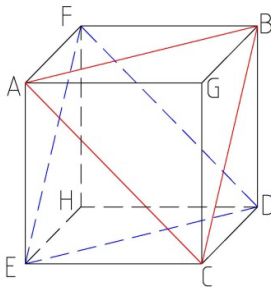


FIGURE 2. The cubic Stewart platform.

In addition, the control ability and stiffness of each direction have the advantage of consistency [11].

Due to the above structural characteristics, the cube-configuration Stewart platform has uniform control of each leg. The sensors installed in the direction along the axis of each leg are orthogonal, as are the vibration signals of each leg. That means we can convert multiple input-output (MIMO) control problems into single-input and output (SISO) control problems [12], [13]. For the vibration reduction of vehicle seats, the vibration control of multiple degrees of freedom can be realized relatively conveniently by using the cubic Stewart mechanism.

Therefore, in this paper, a new structure of an MDOF seating system vibration reduction platform based on the cubic Stewart parallel mechanism is proposed. Next, passive and active vibration control analysis is performed on the structure. The results show that controlling the axial vibration acceleration of each branch leg of the seat platform can greatly reduce the vibration of the seat upper platform in the vertical, horizontal and roll directions simultaneously.

II. SEAT SUSPENSION MODEL

A. KINEMATICS ANALYSIS OF THE CUBIC STEWART PLATFORM

The seating system of the cubic Stewart platform model consists of two platforms and six group U-C-U branching legs. Each leg is connected with the upper and lower plates through the universal pair (U), The upper and lower parts of the branching leg are connected by the cylinder pair (C). The side lengths of the upper and lower platforms are the same, and the angle between any two adjacent branch legs is 90°.

To clearly describe the motion of the seating platform, two coordinate systems are defined, that is, the upper (moving) coordinate system (P-XYZ) and the lower (static) coordinate

system (B-XYZ). The static coordinate system is fixed on the lower platform. The origin is the center of the outer circle of the triangle formed by the three hinge points connected in turn on the lower platform. The moving coordinate system is fixed on the upper platform [14] and moves with the upper platform. The origin is located at the center of the outer circle of the triangle formed by three hinge points connected in turn on the upper platform.

The transformation matrix from the moving platform coordinate system (P-xyz) to the static coordinate system (B-xyz) is follows (1), as shown at the bottom of this page.

In Equation 1, α, β, and γ are the Euler angles of the upper platform, and the relationship between the angular velocity of point P of the upper platform and its Euler angles is as follows:

$$\omega_p = \begin{bmatrix} \omega_{px} \\ \omega_{py} \\ \omega_{pz} \end{bmatrix} = \begin{bmatrix} \cos \beta \cos \gamma & \sin \gamma & 0 \\ -\cos \beta \sin \gamma & \cos \gamma & 0 \\ \sin \beta & 0 & 1 \end{bmatrix} \begin{bmatrix} \dot{\alpha} \\ \dot{\beta} \\ \dot{\gamma} \end{bmatrix} \quad (2)$$

Assuming that the rotation angle between the upper platform and the lower platform is small enough, this equation can be simplified as:

$$\omega_p \approx [\dot{\alpha} \quad \dot{\beta} \quad \dot{\gamma}]^T \quad (3)$$

In the following analysis, t denotes the vector from point Ob (the origin of coordinate system (B-xyz)) to point Op (the origin of coordinate system (P-xyz)), t = (x, y, z), and P = (α, β, γ) is the Euler angle relative to the coordinate (B-xyz).

The connection vector from Op to each leg of the upper platform is pi, and the connection vector from Ob to each leg of the lower platform is bi, so the direction vector of the axis of the six legs of Si and the cubic Stewart platform can be represented by the following formula:

$$S_i(i = 1, 2, \dots, 6) = Rp_i + t - b_i \quad (4)$$

The leg length in this equation is:

$$L_i = \|S_i\| = \|Rp_i + t - b_i\| \quad (5)$$

The unit vector of each leg is:

$$s_i = \frac{S_i}{\|S_i\|} = \frac{(Rp_i + t - b_i)}{\|Rp_i + t - b_i\|} \quad (6)$$

The Jacobian matrix is related to the leg elongation velocity (si) and velocity vector χ = (v^Tω^T)^T, and the attitude of the upper platform is a function of (x, y, z, α, β, γ), where

$$\omega = \dot{\theta}, \quad v = \dot{i}, \quad \dot{\chi} = (v^T \omega^T)^T, \quad q_i = Rp_i \quad (7)$$

$$\begin{aligned} R_{(P/B)} &= Rot(x, \alpha)Rot(y, \beta)Rot(z, \gamma) \\ &= \begin{bmatrix} \cos \beta \cos \gamma & -\cos \beta \sin \gamma & \sin \beta \\ \cos \alpha \sin \gamma + \sin \alpha \sin \beta \cos \gamma & \cos \alpha \cos \gamma - \sin \alpha \sin \beta \sin \gamma & -\sin \alpha \cos \beta \\ \sin \alpha \sin \gamma - \cos \alpha \sin \beta \cos \gamma & \sin \alpha \cos \gamma + \cos \alpha \sin \beta \sin \gamma & \cos \alpha \cos \beta \end{bmatrix} \end{aligned} \quad (1)$$

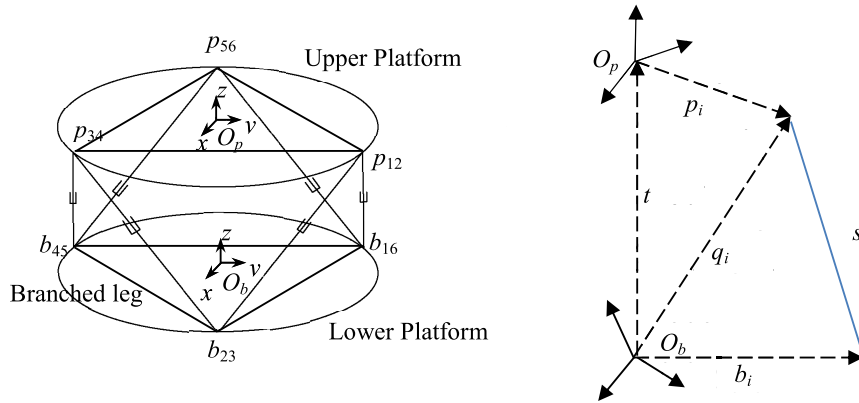


FIGURE 3. Cubic Stewart schematic diagram.

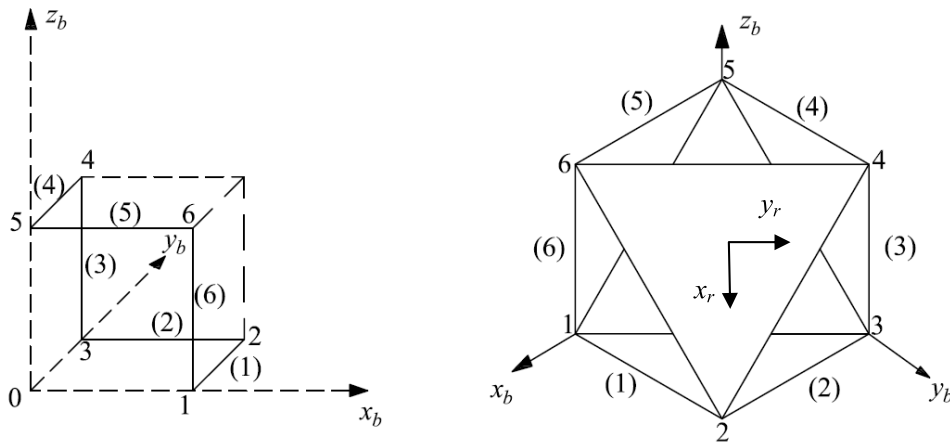


FIGURE 4. Coordinate systems for the dynamic model of the cubic Stewart platform.

The sliding speed of each leg is:

$$\begin{aligned} \dot{S} &= s_i(v + \omega \times q_i) = s_i^T v + s_i^T (\omega \times q_i) = s_i^T v + (q_i \times s_i)^T \omega \\ &= (s_i^T (q_i \times s_i))^T \begin{pmatrix} v \\ \omega \end{pmatrix} = J \dot{\chi} \end{aligned} \tag{8}$$

The Jacobian matrix can be represented as:

$$J = (s_i^T (q_i \times s_i))^T \tag{9}$$

B. DYNAMIC ANALYSIS OF THE CUBIC STEWART PLATFORM

A previous report [15] gives an ideal dynamic modeling method for the Stewart platform. The cubic Stewart platform has been extensively studied because it is orthogonally symmetric. The stiffness of the cubic Stewart platform is consistent with the control capability, and the coupling between actuators is minimal. The supporting legs of the platform are the edges of the cube connecting the points between the lower base platform and the upper load platform. According to the literature [16], the coordinate systems for a dynamic model of the cubic Stewart platform are shown in Fig. 4. The lower platform consists of nodes 1, 3, and 5, and the

upper platform is connected by nodes 2, 4, and 6. The branch legs are the edges of the cube connecting the nodes between the lower and upper platforms. The origin of reference frame $\{x_b, y_b, z_b\}$ of the lower platform is at node 0, and the origin of the reference coordinate system $\{x_r, y_r, z_r\}$ of the upper platform is the geometric center of the Stewart platform (the center of the cube).

Assuming that the lower base platform is fixed, the upper load platform is an axisymmetric rigid body moving platform. The mass of the upper load platform is m , the principal axis of inertia is aligned with $\{x_r, y_r, z_r\}$, the principal moments $I_x = I_y = mR_x^2 = Bf$, and $I_z = mR_z^2$. We also assume that the leg is rigid, and the stiffness of the universal pair is ignored. The second-order differential equation of motion of the seating system model is as follows [16]:

$$M\ddot{x} + Kx = Bf \tag{10}$$

In this equation, $x = (x_r, y_r, z_r, \theta_x, \theta_y, \theta_z)^T$ is the vector of small displacement and rotation under the reference system. $f = (f_1, f_2, f_3, f_4, f_5, f_6)^T$ is the collection of active control force vectors from leg 1 to leg 6. K and M are

the stiffness matrix and mass matrix, respectively. B is the Jacobian matrix.

To establish the equation of motion and find the eigenvalues of the cubic Stewart platform, the estimate of kinetic energy T of the upper platform under $\{x_r, y_r, z_r\}$ is estimated as follows:

$$T = \frac{1}{2}Mv^2 + \frac{1}{2}\omega^T I\omega \quad (11)$$

where M is the 3×3 diagonal mass matrix, v is the translational velocity vector of the center of mass of the moving platform, I is the moment of inertia and ω is the angular velocity of the load. In the reference system, v can be expressed as

$$v = \begin{pmatrix} \dot{x}_r + \dot{\theta}_y Z_c \\ \dot{y}_r - \dot{\theta}_x Z_c \\ \dot{z}_r \end{pmatrix} \quad (12)$$

In the equation, θ rotates in the direction of I , and Z_c is the distance between the center of mass of the moving platform and the origin of the reference system in the direction of Z . Since the principal inertia is aligned with $\{x_r, y_r, z_r\}$, the rotating part is:

$$\omega^T I\omega = I_x(\dot{\theta}_x)^2 + I_y(\dot{\theta}_y)^2 + I_z(\dot{\theta}_z)^2 \quad (13)$$

In this equation, $I_x = I_y = mR_x^2$, $I_z = mR_z^2$, and R_x and R_z are the radii of rotation. The kinetic energy can be calculated by the following formula:

$$T = \frac{1}{2}\dot{x}^T M\dot{x} \quad (14)$$

where M is the global mass/inertia matrix, $x = (x_r, y_r, z_r, \theta_x, \theta_y, \theta_z)^T$ is the global translation and rotation vector, and the general mass matrix can be derived from formula (11) and formula (14) as follows:

$$M = m \begin{pmatrix} 1 & 0 & 0 & 0 & Z_c & 0 \\ 0 & 1 & 0 & -Z_c & 0 & 0 \\ 0 & 0 & 1 & 0 & 0 & 0 \\ 0 & -Z_c & 0 & R_x^2 + Z_c^2 & 0 & 0 \\ Z_c & 0 & 0 & 0 & R_x^2 + Z_c^2 & 0 \\ 0 & 0 & 0 & 0 & 0 & R_x^2 \end{pmatrix} \quad (15)$$

The stiffness matrix K can be calculated by the stiffness formula $[k BB^T]$, as follows:

$$K = k \text{diag} \{2, 2, 2, 0.5L^2, 0.5L^2, 2L^2\} \quad (16)$$

$$B = \frac{1}{\sqrt{6}} \begin{pmatrix} 1 & 1 & -2 & 1 & 1 & -2 \\ \sqrt{3} & -\sqrt{3} & 0 & \sqrt{3} & -\sqrt{3} & 0 \\ \sqrt{2} & \sqrt{2} & \sqrt{2} & \sqrt{2} & \sqrt{2} & \sqrt{2} \\ -0.5L & 0.5L & L & 0.5L & -0.5L & -L \\ -\frac{\sqrt{3}}{2}L & \frac{\sqrt{3}}{2}L & 0 & \frac{\sqrt{3}}{2}L & \frac{\sqrt{3}}{2}L & 0 \\ L\sqrt{2} & -L\sqrt{2} & L\sqrt{2} & -L\sqrt{2} & L\sqrt{2} & -L\sqrt{2} \end{pmatrix} \quad (17)$$

The eigenvalues can be obtained by formula (10), where the mass matrix M , stiffness matrix K and Jacobian matrix B are given by formula (15) to formula (17). The characteristic equations are derived as follows:

$$M\ddot{x} + Kx = 0 \quad (18)$$

$$(Ms^2 + K)x = 0 \quad (19)$$

By solving the matrix equation, the natural frequency of the system is obtained. The z-translation mode and the z-rotation mode are decoupled. Their natural frequencies are given by:

$$\Omega_3 = \sqrt{2}\Omega_0 \quad \Omega_6 = \frac{\sqrt{2}}{\rho_z}\Omega_0 \quad (20)$$

where $\Omega_0 = \sqrt{k/m}$ and ρ_z is the z-axis radius of rotation by the normalized leg length. In most cases, $\rho_z < 1$, and $\Omega_6 > \Omega_3$. The natural frequency is the root of the following equation:

$$\left(2 - \frac{\Omega^2}{\Omega_0^2}\right) \left(\frac{1}{2} - \rho_x^2 \frac{\Omega^2}{\Omega_0^2}\right) - 2\rho_c^2 \frac{\Omega^2}{\Omega_0^2} = 0 \quad (21)$$

In this equation, $\rho_x = R_x/L$ is the x-axis normalized radius of rotation, and $\rho_c = Z_c/L$ is the normalized centroid offset.

C. ADAMS VIRTUAL PROTOTYPE MODEL

The virtual prototype of the cubic Stewart mechanism seating system model was constructed in ADAMS software. It consists of one lower (basic) plate, six branch legs and one upper (load) plate, and the connecting hinge consists of 6 cylinder pairs and 12 universal pairs. Fig. 5 shows the virtual prototype model constructed in ADAMS according to the parameters listed in Table 1.

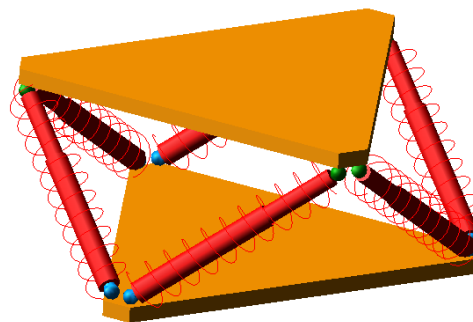


FIGURE 5. The virtual prototype of the seating system model in ADAMS software.

III. MODEL VALIDATION

A. MODEL TEST IN VERTICAL DIRECTION

To verify the accuracy of the virtual prototype model of the seating system, a modal test was carried out on the prototype. In the sitting position, approximately 75% of the body weight is applied on the seat. The test method adds 60 kg load to the upper platform. (Assuming the driver weighs between 65 and 70 kg, the body weight applied on the seat is approximately 50 kg; in addition, 10 kg is added to the seating system

TABLE 1. The main parameters of the seat suspension.

Item	Value
Upper platform mass	2 kg
Lower platform mass	2 kg
Load mass	60 kg
The side length of the upper platform	450 mm
The side length of the lower platform	450 mm
Stiffness of the branch leg	15000 N/m
Damping coefficient of the branch leg	100 N·m/s
Mass of the universal pairs	0.5 kg
Mass of the branch leg	1 kg
Length of the branch leg	318 mm



(a) The prototype of the seat suspension and load



(b) The acceleration sensor arranged at the upper platform

FIGURE 6. (a). The prototype of the seat suspension and load. (b). The acceleration sensor arranged at the upper platform.

suspension as the weight of the cushion and backrest. That is, a total of 60 kg load is applied on the seating system platform.) Then, we lift the seat platform to a certain height and release it. The acceleration signal of the upper platform is measured by an acceleration sensor mounted on the upper platform. The prototype of the cubic Stewart mechanism seating system and the load mass are shown in Fig. 6(a), and the location of the acceleration sensor is shown in Fig. 6(b).

The free attenuation vibration signal of the seating system platform is processed by the time history method, and the natural frequency f of the seating system platform in the vertical vibration mode is calculated according to Equation (22).

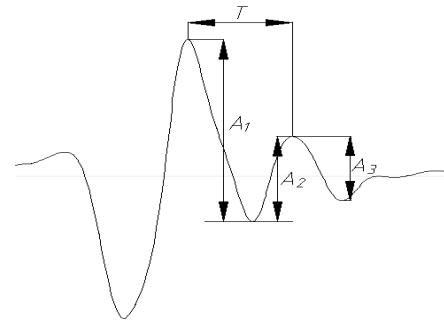


FIGURE 7. Acceleration theoretical attenuation curve.

After the seating system platform lands on the ground, the amplitude of acceleration decays gradually with the time change. Fig. 7 shows the theoretical attenuation curve of acceleration.

$$f = \frac{1}{T} \tag{22}$$

In this equation: T is the vibration period of the upper platform.

The damping ratio can be calculated through the whole-period decay rate $\tau = A1/A3$ (the expression of the theoretical acceleration attenuation curve and the definition $A1$ and $A3$ are shown in Fig. 7) of the acceleration amplitude. The expression of the damping ratio ξ is calculated by the following equation:

$$\xi = \frac{1}{\sqrt{1 + \frac{4\pi^2}{\ln^2 \tau}}} \tag{23}$$

The test result is shown in Fig. 8.

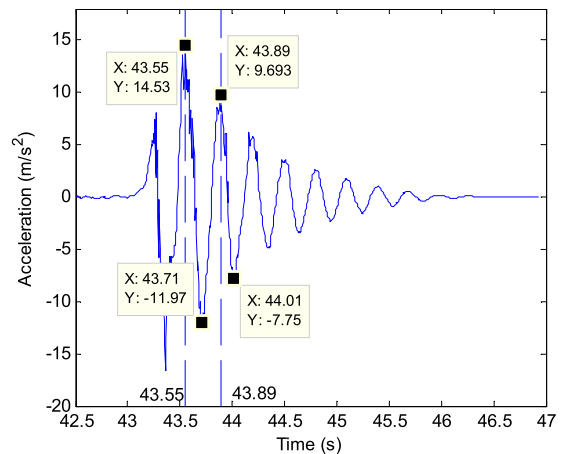


FIGURE 8. The test result of acceleration of upper platform.

As is shown in Fig. 8, the free falling vibration period T of the upper platform of the seat prototype is 0.34 s, so the natural frequency of the seat prototype in the vertical direction is 2.94 Hz. The whole-period decay rate is $\tau = 26.5/17.44 = 1.52$, so the damping ratio ξ of the vertical direction of the seat platform is 0.066.

B. MODEL SIMULATION IN THE VERTICAL DIRECTION

In the model simulation, the vertical input and output channels are established at the center of the lower platform and the center of the upper platform; then, a 1-20 Hz unit acceleration sweep sine excitation was applied in the center of the lower platform. The simulation analysis is carried out in the ADAMS Vibration module, and the acceleration transfer function curve of the vertical direction of the seat model is obtained, as shown in Fig. 9.

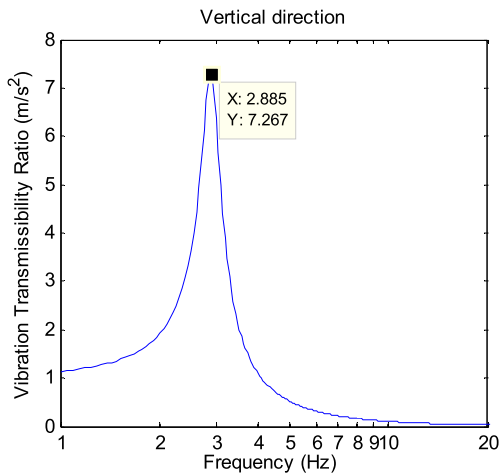


FIGURE 9. The simulation result of the transmissibility ratios of the seat platform in the vertical direction.

As is shown in Fig. 9, the peak value of the vibration transmissibility appears at 2.88 Hz, indicating that the vertical mode natural frequency of the seating system model is 2.88 Hz. This simulation result is very close to the test result of 2.94 Hz. The maximum amplitude of the vibration transmissibility curve is 7.27. The damping ratio of the cubic Stewart mechanism seating system model in the vertical direction can be calculated using Equation (24), the calculated result is 0.069, which is very close to the measured result of 0.066. This proves that the cubic Stewart mechanism seating system model established in ADAMS software is accurate.

$$\xi = \frac{\sqrt{\lambda^4 - \beta^2 (1 - \lambda^2)^2}}{2\lambda\beta} \quad (24)$$

where β is the vibration transmissibility ratio, ξ is the damping ratio and λ is the frequency ratio (when the excitation frequency is equal to the natural frequency, this value is 1).

IV. THE PARAMETER SENSITIVITY ANALYSIS OF THE SEAT SUSPENSION MODEL FOR VIBRATION CONTROL

To analyze the influence of different parameters of the seating system platform on the vibration amplitude, the parameter sensitivity analysis of the stiffness and damping coefficients of the branch legs and the seating system bearing load are carried out in this article using simulation analysis. The bearing load mass, stiffness and damping coefficients of the branch leg are increased and decreased by 10%, respectively.

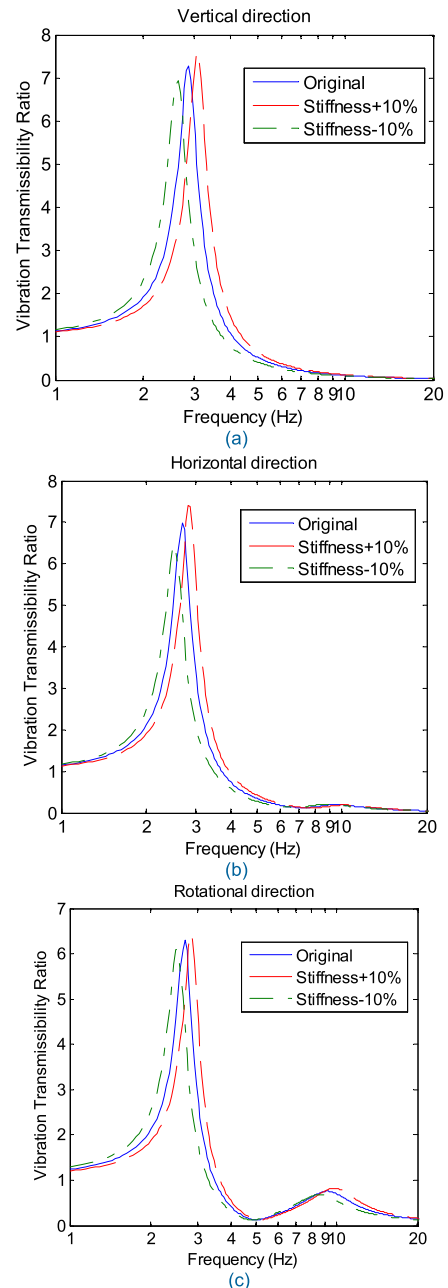


FIGURE 10. Transmissibility ratios of the seating system platform with and without the 10% chain stiffness change. (a). Vertical direction analysis result (b). Horizontal direction analysis result (c). Roll direction analysis result.

First, the stiffness of each branch leg was changed to analyze the sensitivity. The stiffness of each branch leg was increased and reduced by 10%, and the vibration responses of the seat platform in the vertical direction, horizontal direction and roll direction are analyzed. Input and output channels are established in the lower platform center and the upper platform center of the seat platform model, respectively. Frequency sweep excitations of unit acceleration amplitude in the frequency band of 1-20 Hz are applied to the lower platform center in the three directions, and then the vibration

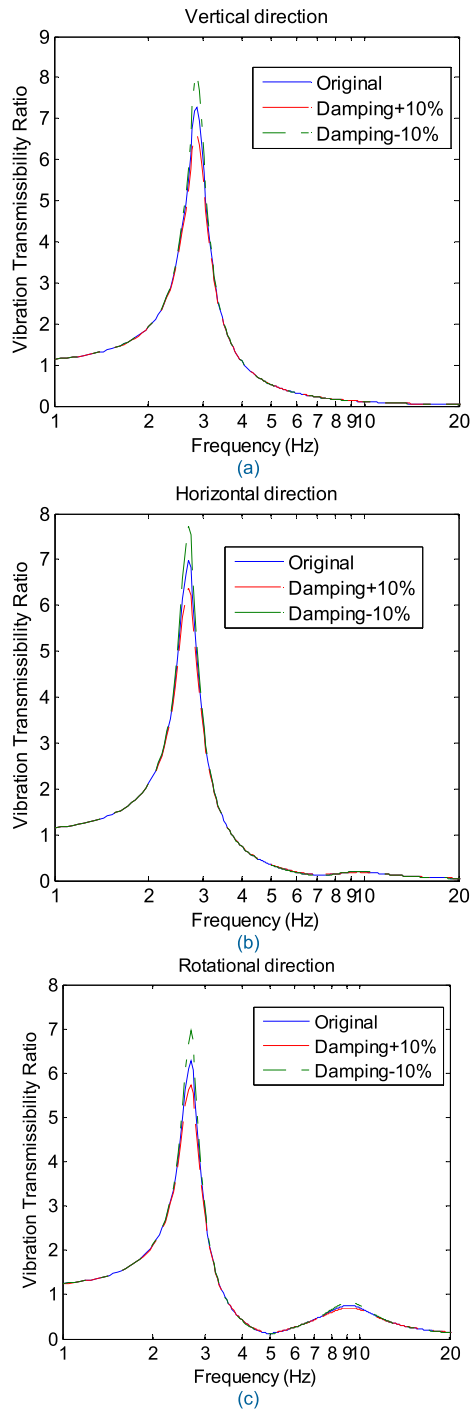


FIGURE 11. Transmissibility ratios of the seating system platform with and without the 10% chain damping coefficient change. (a). The analysis result in the vertical vibration direction (b). The analysis result in the horizontal direction (c). The analysis result in the roll direction.

transfer analysis was carried out. The curves of the acceleration transfer functions under different stiffness conditions are obtained. The analysis results are shown in Fig. 10.

From Fig. 10, it can be found that with the stiffness increases, the natural frequencies of the three modes all increase. In the low-frequency region, the vibration

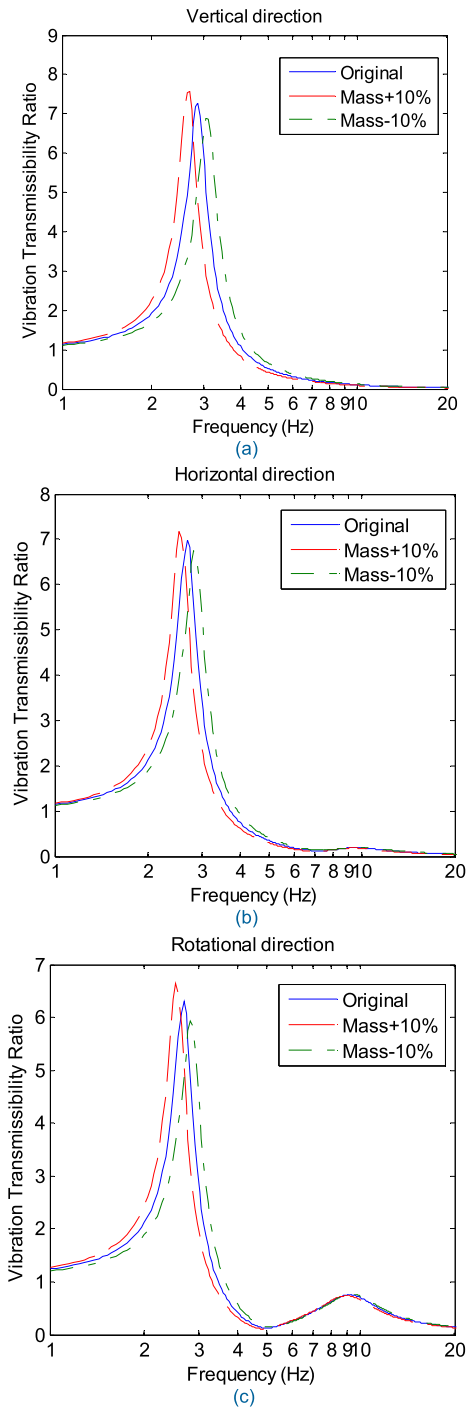


FIGURE 12. The amplitudes of the transmissibility ratios of the seating system platform with and without the 10% load bearing change. (a). The analysis result in the vertical direction (b). The analysis result in the horizontal direction (c). The analysis result in the roll direction.

transmissibility decreases as the stiffness increases, and in the high-frequency region, the transmissibility of vibration increases as the stiffness increases. These results show that in the vibration reduction region (where the vibration transmission rate is less than 1), the vibration attenuation performance of the seating system platform decreases as the stiffness increases.

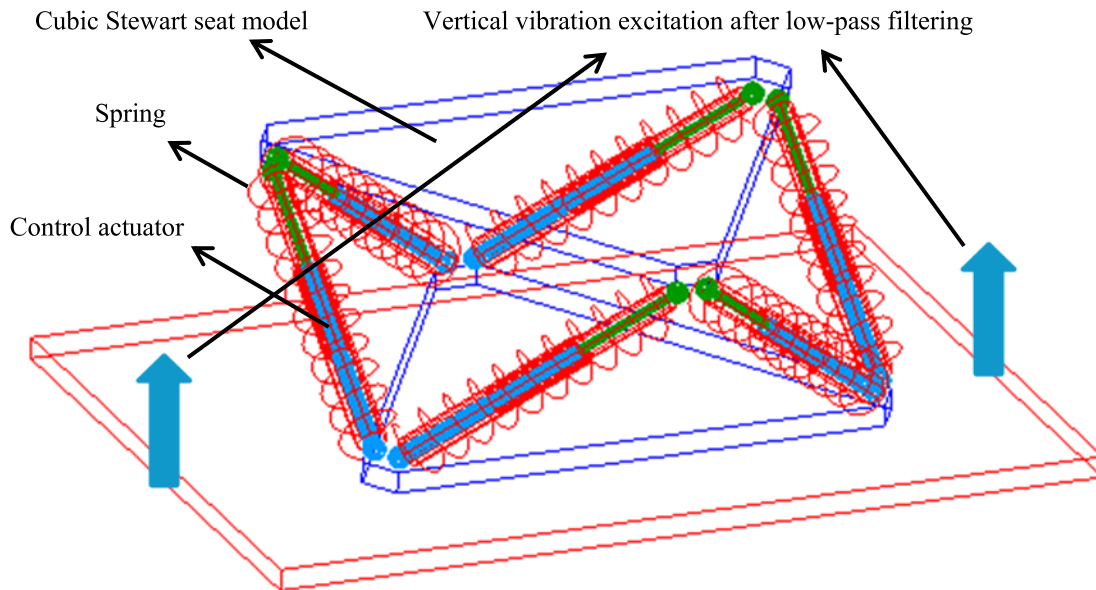


FIGURE 13. Vibration simulation model of the cubic Stewart mechanism seating system platform.

Then, the damping coefficient sensitivity analysis is carried out. The damping coefficient of each branch leg is increased and reduced by 10%. Then, the frequency sweep excitations of the unit acceleration amplitude in the three directions of vertical, horizontal and roll are applied to the lower platform center. The curves of all acceleration transmissibility curves under different damping conditions are shown in Fig. 11.

From Fig. 11, it can be seen that in all three directions, in both the low-frequency region and the high-frequency region, the 10% branch leg damping coefficient change has very little effect on the vibration transmissibility ratio of the seating system platform. Near the resonant frequency, the transmissibility of vibration decreases obviously as the damping coefficient increases. It can be concluded that suitably increasing the damping coefficient of the branch leg can reduce the vibration transmissibility ratio of the seating system platform and improve comfort in the resonant frequency region in all three directions, but in the non-resonant frequency regions, the damping coefficient changes have very little effect on the transmissibility ratio amplitude. In addition, the change in the damping coefficient has little effect on the natural frequency.

Finally, the sensitivity analysis of the bearing load mass is carried out. The bearing load mass of the upper platform is increased and reduced by 10%. Then, the frequency sweep excitations in the unit acceleration amplitude in the three directions are applied to the lower platform center. In addition, the curves of all the acceleration transmissibility ratio amplitude curves under different bearing load masses are shown in Fig. 12.

It can be seen from Fig. 12 that in all three directions of vertical, horizontal and roll, as the bearing load mass increases, the natural frequency decreases, and the vibration

attenuation effect in the vibration reduction region increases. The effect of a bearing load mass change on the vibration acceleration transmissibility is opposite to that of a change in the stiffness of each branch leg, and the effect of a bearing load mass change on the natural frequency is also opposite to that of a change in the stiffness of each branch leg.

V. DESIGN OF ACTIVE VIBRATION CONTROLLER

In the typical design procedure of vibration isolation, to get a good vibration reduction effect, the dominant excitation frequency should be much larger than the natural frequency of the seating suspension system. However, the suspension deflection is too large when the natural frequency of the suspension system is too low. It is difficult to attain a very low natural frequency. Therefore, active vibration control method should be adopted in order to reduce vibration in the low frequency range.

In the cubic Stewart mechanism, the coupling between each leg is minimal. A control actuator can be designed and added to each leg and connected in parallel with springs to realize the combination of active and passive vibration control (shown in Fig. 13). Thus, the vibration acceleration of the upper plate can be reduced in multiple degrees of freedom or directions.

In traditional control engineering, the PID method has become the most widely used method. With the development of modern control theory, many new control methods have been applied in the field of automation control, but because of its simple structure, strong robustness and good stability, the PID controller is still widely used in various fields of industrial control.

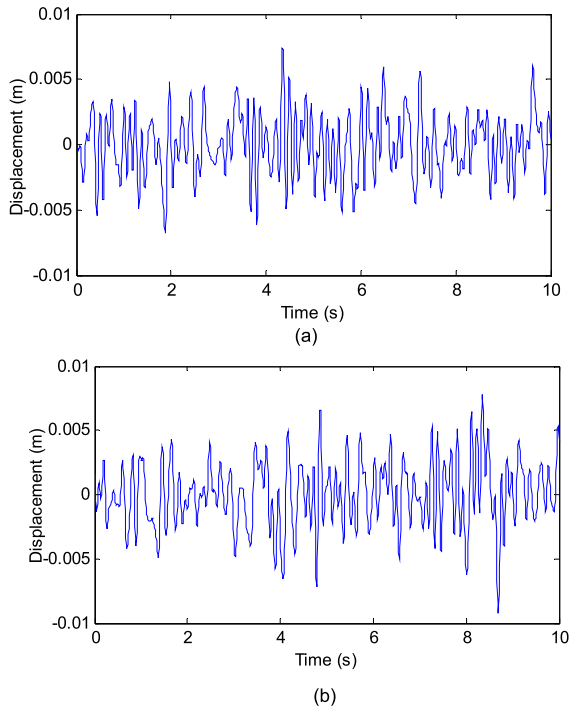


FIGURE 14. The input displacement excitation after low-pass filtering.

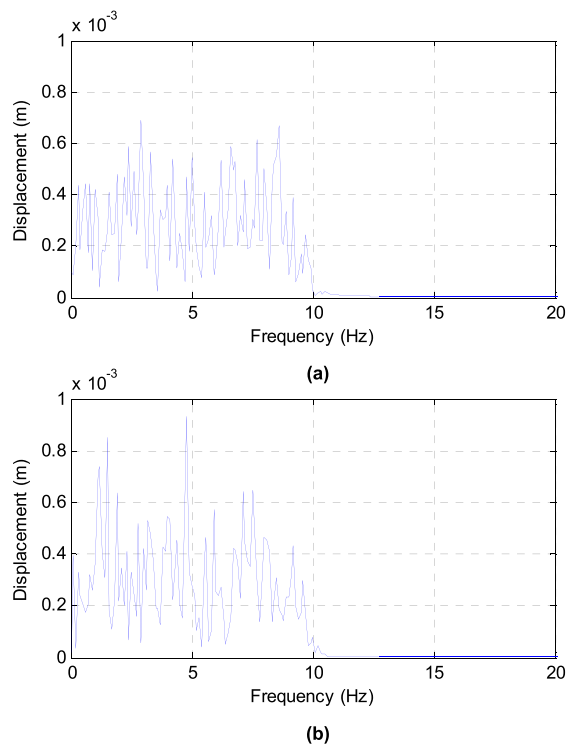


FIGURE 15. The FFT results of the input displacement excitation signals after low-pass filtering.

Therefore, the PID method is employed in this paper and consists of a proportional unit P, an integral unit I, and a differential unit D. The controller is set with three parameters: KP, KI and KD. The PID controller is used for vibration

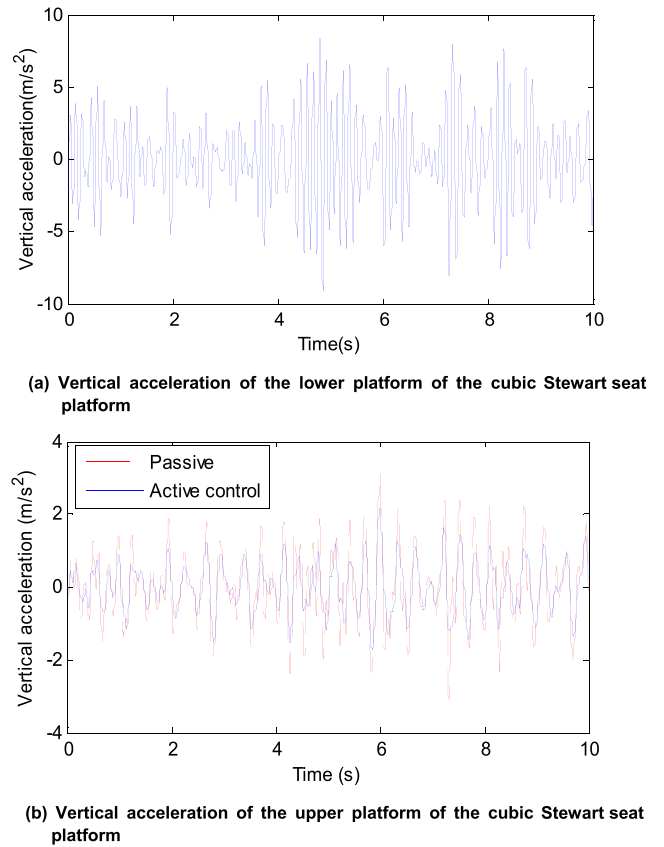


FIGURE 16. (a) Vertical acceleration of the lower platform of the cubic Stewart seat platform. (b) Vertical acceleration of the upper platform of the cubic Stewart seat platform.

control of the cubic Stewart mechanism seating suspension system.

In this paper, the control system is established in MATLAB/Simulink environment. For the cubic Stewart mechanism, the axial acceleration at the center of mass of the six branch legs is taken as the control output variable, the driving force applied on the six legs is taken as the input variable, and the cubic Stewart mechanism seating suspension system model is simulated using Simulink, which is connected to the ADAMS/control module.

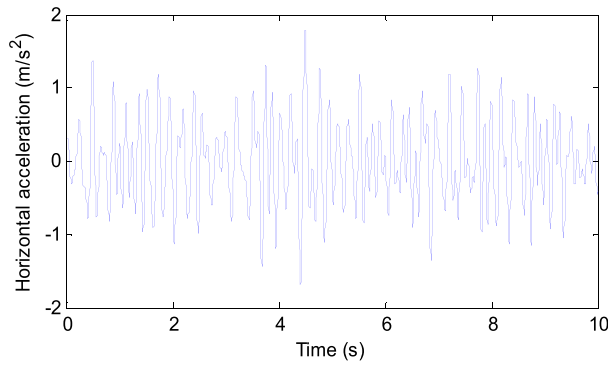
Six PID controllers are applied to the cubic Stewart mechanism seating suspension system; each controller is used to control the axial vibration acceleration of each branch leg.

In this paper, the PID controller sets its control parameters by the trial and error method. The specific process of the adjustment is as follows.

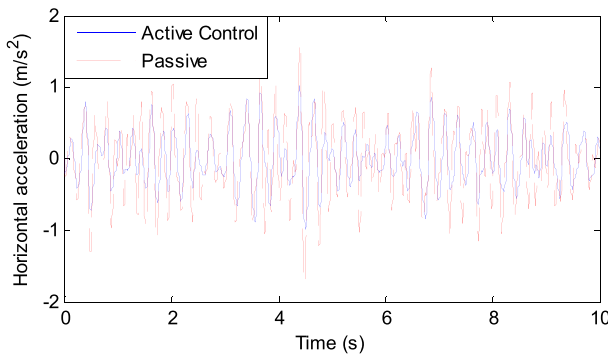
(1) First, adjust parameter KP. Set KI and KD to 0, adjust KP from small to large, and simulate the controller to obtain the best KP value.

(2) Then, adjust KI. Keep the parameter KP at the original value, and then adjust KI step by step from small to large to observe the simulation results in Simulink. When the static error is minimized, record the KI value.

(3) Finally, adjust the parameter KD. The adjustment method is same as the KI method, and the parameters with good control effect are obtained. Finally, the initial control



(a) Horizontal acceleration of the lower platform of the cubic Stewart seat platform



(b) Horizontal acceleration of the upper platform of the cubic Stewart seat platform

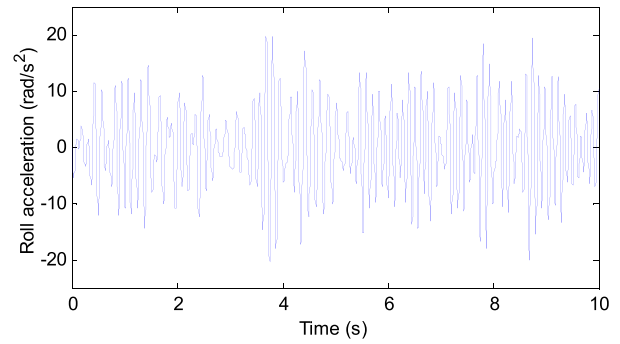
FIGURE 17. (a) Horizontal acceleration of the lower platform of the cubic Stewart seat platform. (b) Horizontal acceleration of the upper platform of the cubic Stewart seat platform.

parameters of the PID controller are found as $K_P = 5$, $K_I = -150$, and $K_D = 0$.

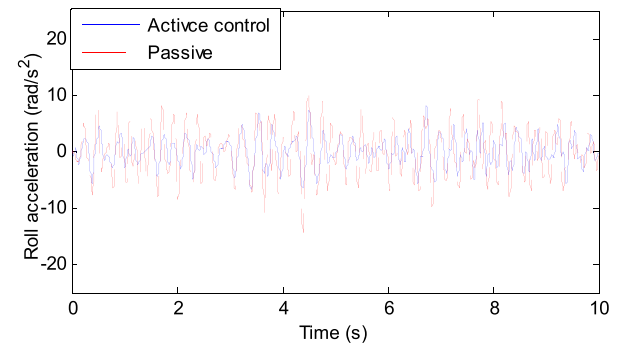
Then, the vibration control simulation of the cubic Stewart mechanism seating suspension system is carried out. Since it has been shown above that the vibration excitation of the seat mainly comes from the excitation of the left and right sides of the vehicle suspension, a plate is placed under the seat during the simulation, and a fixed constraint is applied between the plate and the lower platform under the seat to simulate the condition shown in Fig. 1. Since the vibration excitation signal acting on the floor of the vehicle cab is attenuated by the vehicle suspension, usually below 10 Hz, two random signals are selected in the simulation and passed through a 10 Hz low-pass filter. Then, two segments of such vibration signals are simultaneously applied to both the sides of the lower platform of the seat to simulate the vibration excitation of the cab floor when the vehicle passes over a rough road surface, as shown in Fig. 13.

Two segments of the excitation signal after 10 Hz low-pass filtering are shown in Fig. 14. The FFT results of the two excitation signals are shown in Fig. 15.

Fig. 16 (a)–Fig. 18(a) show the acceleration time traces in the vertical, horizontal and roll directions at the center of the lower platform, and Fig. 16 (b)–Fig. 18(b) show the acceleration time traces of passive and active vibration con-



(a) Roll acceleration of the lower platform of the cubic Stewart seat platform



(b) Roll acceleration of the upper platform of the cubic Stewart seat platform

FIGURE 18. (a) Roll acceleration of the lower platform of the cubic Stewart seat platform. (b) Roll acceleration of the upper platform of the cubic Stewart seat platform.

trol in the vertical, horizontal and roll directions at the center of the upper platform.

From Fig. 16(b)–Fig. 18(b), it can be seen that the amplitudes of the vibration acceleration traces of the upper platform in the vertical, horizontal and roll directions are obviously reduced upon active vibration control. The acceleration RMS values of the lower platform and upper platform under the passive and active vibration controls are shown in Table 2.

TABLE 2. Simulation result.

RMS value	Lower platform	Upper platform		
		Passive	Active control	Reduction (%)
Vertical acceleration(m/s ²)	2.77	0.97	0.68	29.9
Horizontal acceleration(m/s ²)	0.56	0.52	0.36	30.8
Roll acceleration(rad/s ²)	7.24	3.98	2.48	37.7

For passive isolation, the vibration accelerations in all three directions of the cubic Stewart mechanism seating system platform are effectively attenuated. In the vertical, horizontal and rolling directions, 64.9%, 7.1% and 45.0% reductions are achieved, respectively. After the active control method is applied, the vibration amplitudes of the seat platform in the three directions are further reduced. Compared with the

results of the passive vibration control method, the vibration amplitudes in the vertical, horizontal and rolling directions are decreased by 29.9%, 30.8% and 37.7%, respectively after the active vibration control is applied. Under this condition, in the vertical, horizontal and rolling directions, 75.4%, 35.7% and 65.7% vibration reduction effects are achieved, respectively.

VI. CONCLUSION

In this paper, a new multi-degree-of-freedom vibration reduction platform has been proposed based on the cubic Stewart mechanism. A virtual prototype model of the seat vibration reduction platform is designed, and an experiment prototype model is built. Based on the research methods of theoretical modeling, numerical simulation and experiment, both the vehicle passive and active seating suspensions have been studied based on the cubic Stewart parallel mechanism. The following conclusions are reached:

This research develops a new structure of MDOF seating system vibration reduction platform based on the cubic Stewart parallel mechanism, which simplifies the dynamic model of the seat platform and facilitates to realize the MDOF active vibration control of the seating system.

The vibration transmissibility ratio of the seating system platform is very sensitive to the change in the damping coefficients of the branch leg of the seating system platform in the resonant region. The vibration transmissibility ratio is sensitive to the bearing load mass and the stiffness of the branch leg of the seating system platform in the vibration reduction region.

A vibration attenuation method combining active and passive vibration control for reducing the axial vibration of each branch leg of the cubic Stewart mechanism seating system platform is proposed. The analysis results show that in the passive control state, the seating system platform can effectively attenuate the vibrations in the three directions of vertical, horizontal and roll. After the active vibration control method is applied, the vibration reduction effect in all three directions can be further increased.

REFERENCES

- [1] X.-X. Bai, P. Jiang, and L.-J. Qian, "Integrated semi-active seat suspension for both longitudinal and vertical vibration isolation," *J. Intell. Mater. Syst. Struct.*, vol. 28, no. 8, pp. 1036–1049, Aug. 2017.
- [2] X. Wang, F. Bi, and H. Du, "Reduction of low frequency vibration of truck driver and seating system through system parameter identification, sensitivity analysis and active control," *Mech. Syst. Signal Process.*, vol. 105, pp. 16–35, May 2018.
- [3] D. Ning, S. Sun, H. Du, W. Li, and W. Li, "Control of a multiple-DOF vehicle seat suspension with roll and vertical vibration," *J. Sound Vib.*, vol. 435, pp. 170–191, Nov. 2018.
- [4] Z. H. Rahman, J. T. Spanos, and R. A. Laskin, "Multi-axis vibration isolation, suppression, and steering system for space observational applications," *Proc. SPIE*, vol. 3351, pp. 73–81, May 1998.
- [5] A. Preumont, M. Horodincu, I. Romanescu, B. de Marneffe, M. Avraam, A. Deraemaeker, F. Bossens, and A. A. Hanieh, "A six-axis single-stage active vibration isolator based on Stewart platform," *J. Sound Vib.*, vol. 300, nos. 3–5, pp. 644–661, Mar. 2007.
- [6] R. G. Cobb, J. M. Sullivan, A. Das, L. P. Davis, T. T. Hyde, T. Davis, Z. H. Rahman, and J. T. Spanos, "Vibration isolation and suppression system for precision payloads in space," *Smart Mater. Struct.*, vol. 8, no. 6, pp. 798–812, Aug. 1999.
- [7] B. Afzali-Far, P. Lidström, and K. Nilsson, "Parametric damped vibrations of Gough–Stewart platforms for symmetric configurations," *Mechanism Mach. Theory*, vol. 80, pp. 52–69, Oct. 2014.
- [8] L. J. Koutsky and C. T. Brodersen, "Active suspension system for vehicle seats," U.S. Patent 6 059 253 A, May 9, 2000.
- [9] Z. Geng and L. S. Haynes, "Multiple degree-of-freedom active vibration control using a Stewart platform," in *Proc. Int. Conf. Adapt. Struct.*, 1994, p. 499.
- [10] L. Qiaobo, "Analysis and experiment of isolators for micro-vibration active control based on Stewart platform," M.S. thesis, Dept. School Mech. Eng., Shanghai Jiao Tong Univ., Shanghai, China, 2016.
- [11] C. Wang, Y. Chen, and Z. Zhang, "Simulation and experiment on the performance of a passive/active micro-vibration isolator," *J. Vib. Control*, vol. 24, no. 3, pp. 453–465, Aug. 2018.
- [12] Z. J. Geng, G. G. Pan, L. S. Haynes, B. K. Wada, and J. A. Garba, "An intelligent control system for multiple degree-of-freedom vibration isolation," *J. Intell. Mater. Syst. Struct.*, vol. 6, no. 6, pp. 787–800, Nov. 1995.
- [13] Y. Li, X. Yang, H. Wu, and B. Chen, "Optimal design of a six-axis vibration isolator via Stewart platform by using homogeneous Jacobian matrix formulation based on dual quaternions," *J. Mech. Sci. Technol.*, vol. 32, no. 1, pp. 11–19, Jan. 2018.
- [14] G. C. Lu, "Analysis of kinematics and dynamics of 3UPU/PU parallel platform used in automatic wave compensation," *Adv. Mater. Res.*, vols. 1049–1050, pp. 1061–1066, Oct. 2014.
- [15] Y. Chen and J. E. McInroy, "Identification and decoupling control of flexure jointed hexapods," in *Proc. Millennium Conf. Int. Conf. Robot. Automat. Symp. (ICRA)*, vol. 2, Apr. 2000, pp. 1936–1941.
- [16] A. A. Hanieh, "Active isolation and damping of vibrations via Stewart platform," Ph.D. dissertation, Dept. Act. Struct. Lab., Univ. Libre de Bruxelles, Brussels, Belgium, 2003.



FENGRONG BI received the Ph.D. degree in power machinery and engineering from Tianjin University, Tianjin, China. He is currently the Ph.D. Supervisor and a Professor with Tianjin University. His current research interests include the control of vibration and noise and the fault diagnosis of vehicles and power machineries, with specific investigation on excitation mechanism, transfer characteristics, assessment, and control methods of NVH.



TENG MA received the bachelor's degree in vehicle engineering from the Hebei University of technology, and the master's degree in power machine and engineering from Tianjin University, where he is currently pursuing the Ph.D. degree in power machine and engineering with the State Key Laboratory of Engines. His research interests include engine knock control detection based on vibration signals and vibration control of vehicle.



XU WANG received the bachelor's degree in engineering and the master's degree in science from Tianjin University, in 1985 and 1988, respectively, and the Ph.D. degree from Monash University, in 1995.

He is currently a Professor of engineering with RMIT University, a Fellow of the Society of Automotive Engineers, a Fellow of the Institute Engineers, Australia, and a Chartered Professional Engineer (Engineering Executive). He has published two books, 85 journal articles, and 33 conference papers and awarded one ARC Discovery grant and two ARC Linkage grants, three AUTOCRC grants and one DMTC project grant. He was a recipient of one European patent, one German patent, and three Australian Provisional Patents. He was awarded with six SEH teaching prizes and graduated five HDR degree students.



XIAO YANG graduated from Tianjin University, Tianjin, China, where he is currently pursuing the Ph.D. degree in power machine and engineering with the State Key Laboratory of Engines. His current research interests include fault diagnosis and noise reduction of internal combustion engine.



ZHENPENG LV received the B.E. degree from the School of Mechanical Engineering, Qingdao University, in 2017. He is currently pursuing the M.E. degree with the School of Mechanical Engineering, Tianjin University. His research interest includes active and semi-active control damping seat of vehicle.

• • •